OPEN-LOOP CONTROL OF QUANTUM PARTICLE MOTION: EFFECTIVE SPLITTING IN MOMENTUM SPACE

Babar Ahmad[1], Sergei Borisenok[1,2], Saifullah[1], Yuri Rozhdestvensky[3]

[1]School of Mathematical Science, GC University, Lahore, Pakistan
[2] Department of Physics, Herzen State University, St. Petersburg, Russia
[3] Institute of Laser Physics, St. Petersburg, Russia

ABSTRACT. In this paper an effective quantum particle beam-splitter in the momentum space is realized in the frame of open-loop control scheme. We demonstrate for small interaction time that the splitting effect $\pm 40\hbar k$ with summarized relative intensity in both main components is about 50 per cent from initial intensity of the atomic beam.

Key words : Open-loop control, beam splitter.
AMS Subject Classification : 35B30, 35B37.

1. INTRODUCTION

In nano-lithography the optical control of atomic motion is one of the main problems. In principle, we can make such a control for atom dynamics because there is an exchange of momentum between the atoms and the optical fields. The momentum exchange can be created with practical devices: atomic mirrors and atomic beam splitters which are main elements of atomic interferometer. The most interesting possibility here is to obtain the splitting of the initial atomic wave packet coherently into two main momentum components only by controllable way. It is needed both for increasing of atomic interferometer sensitivity and for the creation of periodic nano-structures by atomic wave packet lithography [1]. Previously, successful splitting of an atomic wave packet has been achieved by using Raman pulses, magneto-optical beam splitter, diffraction in an optical standing wave, adiabatic passage. More recently, coherent splitting has been realized by scattering of an atomic wave packet in standing wave with modulated intensity [2] and by using chirped standing wave fields [3].
In this paper we concentrate on the possibility to split an atomic wave packet in standing wave with modulated amplitude because this beam-splitter has a number of advantages by comparing with others. The first one is the simplicity for an experimental realization because it is quite easy to obtain the time modulation of intensity with any shape. The second advantage is that

the scale splitting of an atomic wave packet can be controlled by changing the values of both an amplitude and the frequency of the modulation. Actually, we demonstrate for small interaction time, which is required for clear and large splitting, the beam-splitting effect $\pm 40\hbar k$ with summarized relative intensity in both main components about 50 per cent from initial intensity of the atomic beam.

The principal opportunity to split the beam in the momentum space was demonstrated in [4]. To achieve the effective splitting, we apply the scheme of open-loop control, or feed-forward control, i.e. a control signal depends only on the time. Our control goal is to obtain the large angle splitting for the initial wave packet after some time of the interaction between the atoms and the field of modulated standing wave.

2. Physical background and mathematical model for beam splitting in the momentum space

Atom lithography is an active field now a days. The resolution of an optical lithography technology is limited by diffraction, which for the case of deep ultraviolet light approaches 200 nm. The progress of recent device technology requires smaller patterning of 10 nm size. However, when one tries to make very small devices, the resolution of the resistance is limited by the spread of the secondary electron in an electron beam lithography, as well as in X-ray lithography.

The ability to generate ultracold atoms using lasers has opened up new possibilities. The long de Broglie wave of cold atoms makes possible an interferometric manipulation with atomic wave packets, which is designed by an optical standing wave. In this case, atoms can be controlled directly to form a desired pattern. To produce the pattern with high resolution, we need to split the wave packet into two coherent momentum components only. For the model with only two states (i.e. an approximation of two level atom states), we have to split the population of the lower state (because the population of the exited state usually loses the coherency very fast by spontaneous decay) in several momentum components (in an ideal case – only two). At the same time to form the pattern with small step we need to control the scale of splitting between two main coherent components in momentum space. Therefore, an atomic beam splitter is the main element for the practical realization of nano-scale lithography with the controlled step by coherent scattering of an atomic wave packet.

Let's consider now a two level atom in a far detuned standing wave with the intensity modulated in time as $I = I_0 f(\varepsilon, \Delta \cdot t, \phi_0)\cos(kx)$, where ε is an amplitude, Δ is the frequency of the modulation, and ϕ_0 is an initial modulation phase. The standing wave with the frequency ω_1 applies between two states of atom system, where the state 1 is ground and the state 2 is the exited one. Here, ω_0 is the frequency of atom transition and the difference

$\omega_1 - \omega_0$ is the detuning. We will assume that the beam from an atom source propagates along z-axis and crosses the optical wave, standing along x-axis, by right angle. The spontaneous emission from the upper level in this system can not be neglected. After some time t of the interactions between the atoms and the field of the standing wave, the initial atomic wave packet is splitted in few coherent momentum components.

Dynamics of the atom in the modulated standing wave is described with nonstationary Schrödinger equation for the wave function $\Psi(r, t)$ of the two level atom:

$$i\hbar\frac{\partial \Psi(r, t)}{\partial t} = \hat{H}\Psi(r, t), \tag{1}$$

where $\hat{H}$ is a Hamiltonian which takes into account both the atom movement along the standing wave and the dipole interaction between the atom and the optical field. For sufficiently large detuning, when it is much larger than Rabi frequency and the natural width of the atomic transition, $\Omega >> R_0, \Gamma$ (where R_0 is the Rabi frequency, Γ is the natural width of the transition), the excited state 2 can be adiabatically eliminated. As the result, we obtain the equation for the amplitude of the probability of the ground state $\Psi_1(x, t)$:

$$i\hbar\frac{\partial \Psi_1(x, t)}{\partial t} = -\frac{\hbar^2}{2m}\triangle_{xx}\Psi_1(x, t) + \frac{R_0^2}{\Omega}[f(\varepsilon, \Delta \cdot t, \phi_0)]^2\cos^2(kx)\Psi_1(x, t), \tag{2}$$

and m is the atom mass.

After the Fourier transform the same equation in the momentum space is given by:

$$i\frac{\partial \Psi_1(p, \tau)}{\partial \tau} = (p^2 + R^2)\Psi_1(p, \tau) + \frac{R^2}{2}\left[\Psi_1(p + 2, \tau) + \Psi_1(p - 2, \tau)\right], \tag{3}$$

where $R^2 = \frac{R_0^2}{2\Omega\omega_R}[f(\varepsilon, (\Delta/\omega_R) \cdot \tau, \phi_0)]^2$, $\omega_R = \hbar k^2/2m$ is called a recoil frequency, $\tau = \omega_R t$. Here we normalized atom momentum along x-axis to $\hbar k$ and the other quantities (the interaction time, the Rabi frequency and the detuning) we normalized to the recoil frequency ω_R. We have to point out that equations (2)-(3) are valid in the approximation when both the changing of atom momentum along z-axis and the initial value along x-axis can be neglected.

3. Shell model for the splitting process: parametric control

To explain the effect of splitting in the momentum space we start from the case of parametric control with a constant R. We invent a complex shell model for Ψ_1-function. Initially the atomic beam has a Gaussian distribution centered at $p = 0$. Thus, from the structure of the RHS (3) we can expect the non-zero meanings of Ψ_1 functions to be concentrated in the neighborhoods of the points $p = 2n$, where $n = 0, \pm1, \pm2, ...$ Then we can predict the

continuous dependency on p with the discrete number n: $\Psi_1(p + 2n, \tau) = y_n(\tau)$. Dynamics Eq. (3) can be re-written in the form:

$$i\frac{dy_n(\tau)}{d\tau} = (4n^2 + R^2)y_n(\tau) + \frac{R^2}{2}\left[y_{n-1}(\tau) + y_{n+1}(\tau)\right] \tag{4}$$

with the initial conditions: $y_0(0) = 1$ $y_{n\neq0}(0) = 0$. Now we want to limit our shell number. In the case of three shells only Eq. (4) becomes very simple:

$$i\frac{dy_0(\tau)}{d\tau} = R^2 y_0(\tau) + R^2 y_1(\tau); \tag{5}$$

$$i\frac{dy_1(\tau)}{d\tau} = (R^2 + 4)y_1(\tau) + \frac{R^2}{2}y_0(\tau).$$

We demand for the elder shells : $y_{\pm2} = y_{\pm4} = ... \equiv 0$ for any moment τ. Eq. (5) can be easily solved:

$$y_0(\tau) = \mathrm{e}^{-i(R^2+2)\tau}\left[C_1\mathrm{e}^{i\omega\tau} + C_2\mathrm{e}^{-i\omega\tau}\right]; \tag{6}$$

$$y_1(\tau) = \frac{1}{R^2}\mathrm{e}^{-i(R^2+2)\tau}\left[-(\omega - 2)C_1\mathrm{e}^{i\omega\tau} + (\omega + 2)C_2\mathrm{e}^{-i\omega\tau}\right],$$

with $\omega = \sqrt{2R^4 + 16}/2$. For the initial conditions $y_0(0) = 1$ and $y_1(0) = 0$ the constants are: $C_1 = (\omega+2)/2\omega$ and $C_2 = (\omega-2)/2\omega$. The corresponding population amplitudes of the shells 0 and ±1 are given by:

$$a_0(\tau) = y_0(\tau)y_0^*(\tau) = 1 - \frac{R^4}{R^4 + 8}\sin^2\left(\frac{\sqrt{2R^4 + 16}\tau}{2}\right); \tag{7}$$

$$a_1(\tau) = y_1(\tau)y_1^*(\tau) = \frac{R^4}{2R^4 + 16}\sin^2\left(\frac{\sqrt{2R^4 + 16}\tau}{2}\right).$$

Surely, the normalization $a_0 + a_{-1} + a_{+1} = a_0 + 2a_1 = 1$ is saved for any moment τ. Now we can see that in the 3-shell model the regular splitting is realized when the time $\tau = (2k + 1)\pi/\sqrt{2R^4 + 16}$, $k = 0, 1, 2, ...$ The same effect can be reproduced in the case of five shells. To simplify the final expression we will omit the coefficients 4 and 16 in RHS, because the numerical meaning of R^2 is about 300 (i.e. $R^2 >> 4$ and 16). Then we apply Laplace transform:

$$i(sY_0(s) - 1) = R^2 Y_0(s) + R^2 Y_1(s)$$

$$isY_1(s) = R^2 Y_1(s) + \frac{R^2}{2}[Y_0(s) + Y_2(s)] \tag{8}$$

$$isY_2(s) = R^2 Y_2(s) + \frac{R^2}{2}Y_1(s).$$

Then:

$$Y_0(s) = \frac{\left(s + \frac{3}{2}iR^2\right)\left(s + \frac{1}{2}iR^2\right)}{\left(s + iR^2\right)\left(s + \frac{2-\sqrt{3}}{2}iR^2\right)\left(s + \frac{2+\sqrt{3}}{2}iR^2\right)}$$

$$Y_1(s) = -\frac{iR^2}{2\left(s + \frac{2-\sqrt{3}}{2}iR^2\right)\left(s + \frac{2+\sqrt{3}}{2}iR^2\right)} \ ; \tag{9}$$

$$Y_2(s) = -\frac{R^4}{4(s + iR^2)\left(s + \frac{2-\sqrt{3}}{2}iR^2\right)\left(s + \frac{2+\sqrt{3}}{2}iR^2\right)} .$$

With the inverse Laplace transform we restore the time-dependent solution in the momentum space:

$$y_0(\tau) = \frac{1}{3}\left[\exp(-iR^2\tau) + \exp\left(-\frac{iR^2\tau}{2(2 + \sqrt{3})}\right) + \exp\left(-\frac{iR^2\tau}{2(2 - \sqrt{3})}\right)\right]$$

$$y_1(\tau) = \frac{\sqrt{3}}{6}\left[\exp\left(-\frac{iR^2\tau}{2(2 - \sqrt{3})}\right) - \exp\left(-\frac{iR^2\tau}{2(2 + \sqrt{3})}\right)\right] \tag{10}$$

$$y_2(\tau) = -\frac{1}{3}\exp(-iR^2\tau) + \frac{1}{6}\left[\exp\left(-\frac{iR^2\tau}{2(2 + \sqrt{3})}\right) + \exp\left(-\frac{iR^2\tau}{2(2 - \sqrt{3})}\right)\right] .$$

The amplitudes are harmonical:

$$a_0(\tau) = y_0(\tau)y_0^*(\tau) = \frac{1}{9}\left[1 + 2\cos\left(\frac{\sqrt{3}}{2}R^2\tau\right)\right]^2$$

$$a_1(\tau) = y_1(\tau)y_1^*(\tau) = \frac{1}{3}\sin^2\left(\frac{\sqrt{3}}{2}R^2\tau\right) \tag{11}$$

$$a_2(\tau) = y_2(\tau)y_2^*(\tau) = \frac{1}{9}\left[1 - \cos\left(\frac{\sqrt{3}}{2}R^2\tau\right)\right]^2 .$$

Surely, again the normalization $a_0 + a_{-1} + a_{+1} + a_{-2} + a_{+2} = a_0 + 2a_1 + 2a_2 = 1$ is satisfied. The splitting effect is obtained, when $\cos(\sqrt{3}R^2\tau/2) = -1$, then the population of the ±2 shells is: $2a_2 = 8/9$, and in the same time $a_1 = 0$ and $a_0 = 1/9$ only (see Fig.1).

However, if the number n of a shell is increased such that $4n^2 >> R^2$ (i.e. for $R \simeq \sqrt{300}$ we have $n >> 10$), then R^2 in (4) can be excluded as a small parameter, and for the elder shells

$$i\frac{dy_n(\tau)}{d\tau} \simeq 4n^2 y_n(\tau) \quad (n >> 10) . \tag{12}$$

This function is almost independent of the neighbor shells and it has the solution
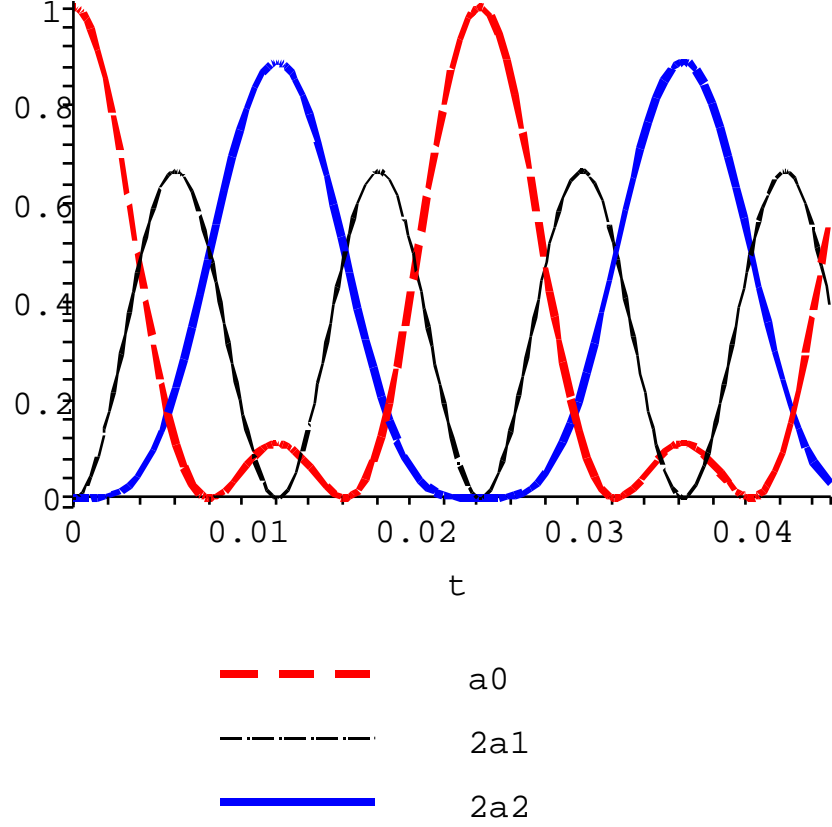
$$y_n(\tau) \simeq e^{-4in^2\tau}y_n(0) . \tag{13}$$

FIGURE 1. Splitting effect for the model of 5 shells.

But $y_n(0) = 0$ for any $n \neq 0$, thus, the elder shells do not participate in the re-distribution of the initial Gaussian population. Thus, the simple parametric control with the fixed R is not enough to split the beam efficiently. Another scheme of time-dependent R (corresponding to the most general open-loop control) should be applied.

4. NUMERICAL SIMULATION RESULTS FOR OPEN-LOOP CONTROL WITH HARMONICAL MODULATION

Now let us consider the two level atom in a far detuned standing wave with an intensity, which is modulated in time harmonically as $I = I_0(1 + \varepsilon\cos(\Delta t))^2\cos^2(kx)$, where ε is the amplitude and Δ is the frequency of the modulation.

We assume also that an initial wave function $\Psi_1(p, \tau = 0)$ has Gaussian

profile with the width δp:

$$\Psi_1(p, \tau = 0) = \frac{1}{\sqrt{2\pi}}\exp\left[-\frac{p^2}{(\delta p)^2}\right]. \tag{14}$$

We remind that now we use the dimensionless time $\tau = \omega_R t$. Fig.2 shows the numerical solution of an equation for amplitude of the probability of ground state $|\Psi_1(p,\tau)|^2$ in momentum representation for the cases unmodulated and modulated standing wave. We assume that initial wave packet has the width equals $\delta p = 0.5\hbar k$ and $\varepsilon = 0.8$, $\Delta/\omega_R = 29$. As we can see from this picture, the scattering result strongly depends on the amplitude modulation exiting in this system. If for an unmodulated case, it is well-known scattering picture observed (Fig.2), when an initial wave packet is splitted into a number of momentum components. However, for modulated standing wave the scattering picture is changing dramatically and two main momentum components centered on $\pm 40\hbar k$ can be observed (Fig.3). Such behavior of the momentum components is due to specific parametric resonance, which occurs in this system by the well defined amplitude and frequency modulation. We have to point out that the values of the modulation obtained for the amplitude and frequency modulation are strongly different from [2], and we can interpret such resonances as Bragg resonances of high orders in modulated standing wave.
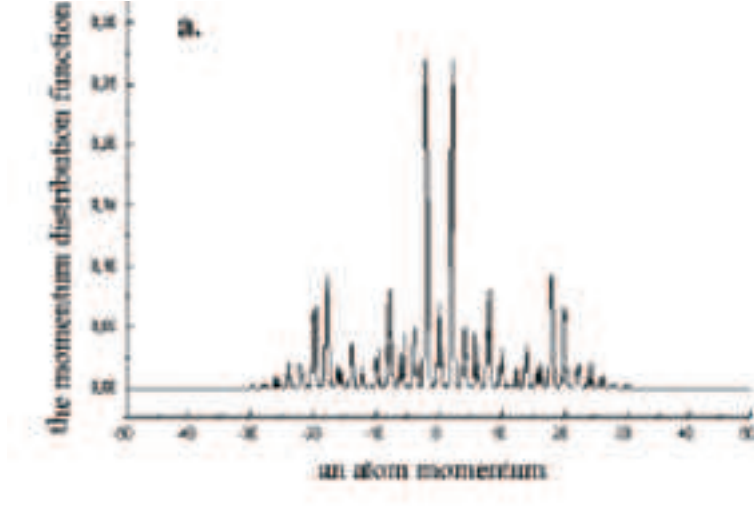

FIGURE 2. The dependence of the distribution function on an atom momentum for an interaction time $\tau_{\text{int}} = 0.567$. The unmodulated standing wave with the dimensionless Rabi frequency $R_0 = (320)^{1/2}$.
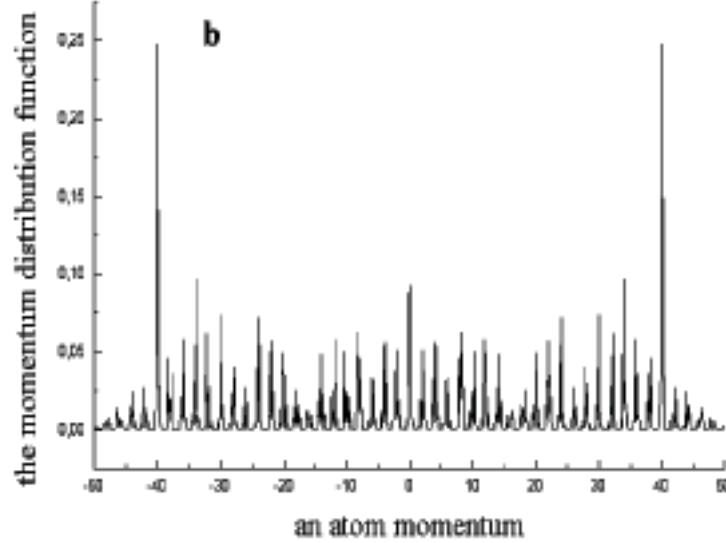
FIGURE 3. The dependence of the distribution function on an atom momentum for an interaction time $\tau_{\text{int}} = 0.567$. The modulated standing wave with the dimensionless Rabi frequency $R_0 = (280)^{1/2}$.

5. Acknowledgment

References

[1] Atom Interferometry. Edited by P. R. Berman. Academic Press, New York, 1997.
[2] A. G. Truscott, M. E. J. Friese, W. K. Hensinger, H. M. Wisemann, H.Rubinsztein-Dunlop, N.R.Heckenberg. *Phys. Rev. Lett.* **84**, 4023 (2000).
[3] V. S. Malinovsky, P. R. Berman. *Phys. Rev. A* **68**, 023610 (2003).
[4] S. V. Borisenok, Yu. V. Rozhdestvensky. Coherent atomic beam-splitter control for nano-scale atom wave packet lithography. 2003 International Conference "Physics and Control", St. Petersburg, Proceedings. P. 906-908 (2003).